Projectile-energy dependence of intensity ratio of $L\alpha$ to L_l x rays produced by proton and ^{3}He impacts on Ho and Sm

M. Kamiya, Y. Kinefuchi, H. Endo,* and A. Kuwako
Department of Physics, Faculty of Science, Tohoku University, 980 Sendai, Japan

K. Ishii and S. Morita
Cyclotron and Radioisotope Center, Tohoku University, 980 Sendai, Japan

(Received 4 April 1979)

The L x rays of Ho and Sm produced by proton and ^{3}He impacts were measured with a Si(Li) detector over the incident energy ranges $E_p = 0.75$–4.75 MeV and $E_{^3\mathrm{He}} = 1.5$–9.3 MeV in the direction of 90° to the projectile. Ratios of x-ray-production cross sections for the $L\alpha$ and L_l lines depend markedly on projectile energy but are independent of the projectile charge. It is shown that these experimental results are in good agreement with the plane-wave-Born-approximation calculation taking into account the effect of inner-shell alignment.

I. INTRODUCTION

As $L\alpha$ and L_l x-ray lines correspond to the transitions $2p_{3/2}$-$3d_{3/2,5/2}$ and $2p_{3/2}$-$3s_{1/2}$, respectively, and come from a vacancy in the $2p_{3/2}$ state (L_3 subshell), it is expected that the ratio of total production cross sections for these two lines is expressed by the corresponding ratio of radiative transition probabilities and must be independent of the projectile energy. Some[1–4] of the experimental results previously obtained on the $L\alpha/L_l$ ratio are independent of the incident proton energy within the experimental errors of about 10% and are in agreement with ratios of theoretical radiative widths calculated by Scofield.[5,6] However, some other experimental results[7–10] show a marked projectile-energy dependence beyond the experimental errors. It must be noted that all of these measurements were in the direction of 90°, assuming isotropic distributions for the characteristic x rays.

In the case of electron-impact ionization, it has been observed that angular distributions of these characteristic x rays and Auger electrons are anisotropic and are dependent on the incident energy.[11–13] This energy dependence of the angular distribution was first pointed out by Mehlhorn[11] and was explained in terms of the dependence of the ionization cross section on the magnetic substate of the orbital electron to be ionized.[14] This results in anisotropic distributions of the characteristic x rays and Auger electrons,[15] and gives rise to a projectile-energy dependence of the ratio of differential cross sections. In the case of heavy-charged particle impact the energy dependence of the differential cross-section ratio $L\alpha/L_l$ may also be understood in terms of this inner-shell alignment effect. Indeed, recently Rødbro *et al.*[16] and Berezhko *et al.*[17] have observed the energy dependence of the alignment probability for Mg L_3-Auger electrons produced by proton and helium-ion impacts.

In the case of an x-ray measurement, the measured x-ray intensity must generally be corrected for absorption in the target and in the air path or the detector window, and therefore highly accurate absolute intensities are difficult to determine. On the other hand, the measurement of the ratio $L\alpha/L_l$ at a fixed angle as a function of incident energy can be carried out with a fixed detection geometry and hence the relative change of the ratio $L\alpha/L_l$ with projectile energy can be measured with high accuracy.

In the present work targets of Sm and Ho were bombarded by proton and ^{3}He-ion beams, and the ratios $L\alpha/L_l$ were measured in the direction of 90° as a function of projectile energy. The ratios $L\alpha/L_l$ as a function of projectile energy are calculated from the plane-wave Born approximation (PWBA) taking into account the alignment of magnetic substates and using nonrelativistic hydrogen-like wave functions, which are expected to be good approximations for L-shell electrons of these high atomic-number targets. The predicted dependence of the ratio $L\alpha/L_l$ on projectile energy, which results from the change of the angular distribution, will be compared with the experimental results.

II. EXPERIMENTAL

A Sm target of 197-μg/cm^2 thickness was self-supporting and a Ho target of 466-μg/cm^2 thickness was prepared by vacuum evaporation onto a thin carbon backing foil. These thicknesses were measured by the Rutherford scattering of protons or ^{3}He ions. The targets were bombarded by pro-

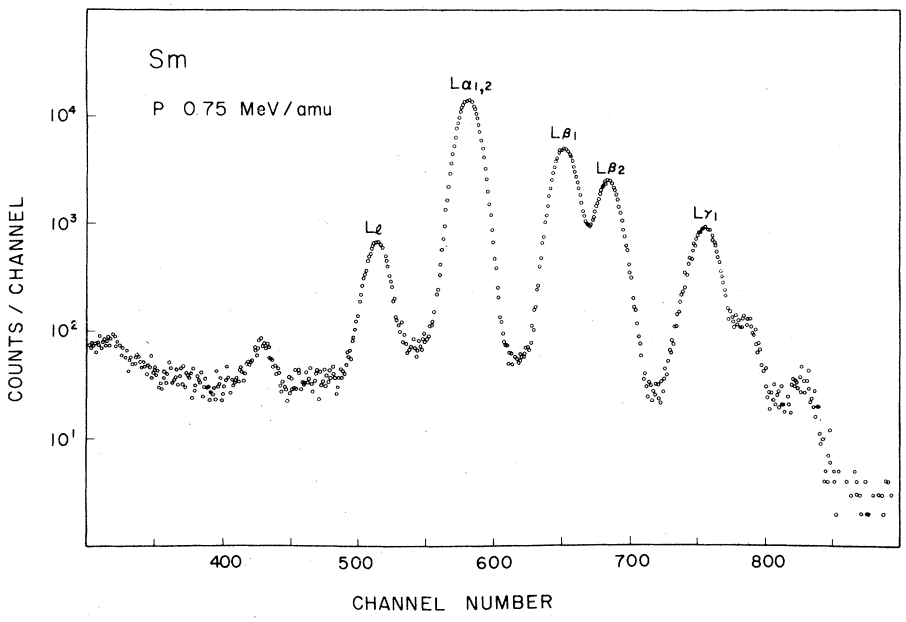

FIG. 1. Typical spectrum of Sm L x rays produced by 0.75-MeV proton impact.

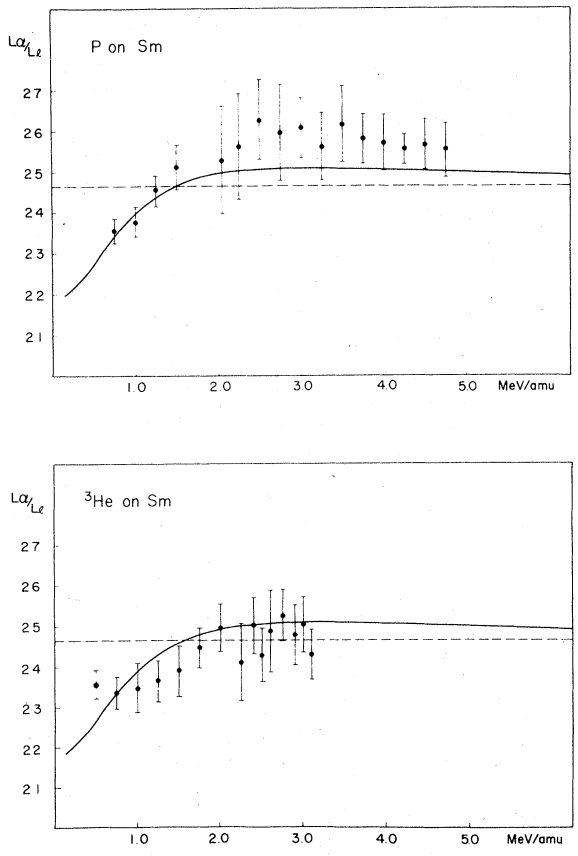

FIG. 2. Intensity ratio $L\alpha/L_l$ for proton and ^{3}He impacts on Sm as a function of projectile energy divided by projectile mass number. Solid lines represent the present theoretical calculation and dashed lines show the value of $\Gamma^{L\alpha}/\Gamma^{L_l}$ calculated by Scofield.

ton beams of 0.75–4.75 MeV and ^{3}He-ion beams of 1.5–9.3 MeV from a 5-MV Van de Graaff generator. The L x rays from the targets were measured in the direction of 90° with an ORTEC Si (Li) detector having an energy resolution of 160 eV for 6.4-keV x rays. As the geometry of experimental setup had been fixed during the measurement, corrections for absorption of x rays had no affect on the excitation curve of the ratio $L\alpha/L_l$. In order to avoid pileup, counting rates were kept below 200 counts per second and sufficient counts were accumulated to obtain the desired statistical accuracy for the L_l peak. In Fig. 1 is shown a spectrum of $L\alpha$ and L_l x-ray lines obtained by 0.75-MeV proton impact on Sm. After subtracting the background, yields of $L\alpha$ and L_l lines were determined by least-squares fitting. Relative errors in the ratio $L\alpha/L_l$ were estimated to be about 4% from the statistical uncertainty of 1% and mainly from the uncertainty in background subtraction. The experimental results are shown in Figs. 2 and 3 for Sm and Ho, respectively.

III. THEORETICAL

Theoretical calculations of inner-shell alignment were first reported by Mehlhorn[11] and developed by Cleff and Mehlhorn,[12] McFarlane,[13] and by Berezhko and Kabachnik.[14] By using hydrogenlike wave functions and the PWBA, the alignment probability has been calculated by McFarlane.[13] According to Berezhko and Kabachnik,[14] angular distributions $W(\theta)$ of $L\alpha$ and L_l x rays emitted from aligned atoms are expressed by

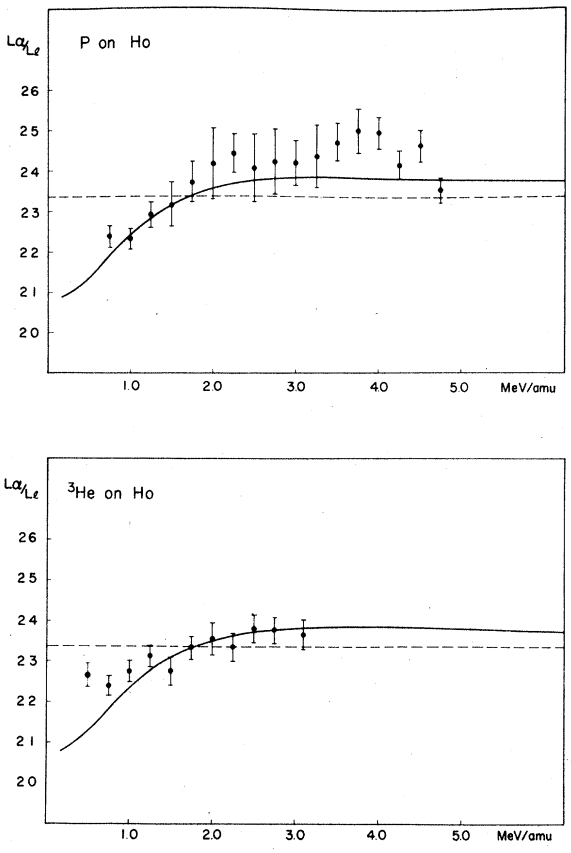

FIG. 3. Same as Fig. 3 except for Ho.

$$W_{L\alpha_1}(\theta) = (W_{L\alpha_1}/4\pi)[1+\tfrac{1}{10}A_2P_2(\cos\theta)],$$

$$W_{L\alpha_2}(\theta) = (W_{L\alpha_2}/5\pi)[1-\tfrac{2}{5}A_2P_2(\cos\theta)], \qquad (1)$$

and

$$W_{L_1}(\theta) = (W_{L_1}/4\pi)[1+\tfrac{1}{2}A_2P_2(\cos\theta)],$$

where $\theta = 0°$ means the incident direction, $P_2(\cos\theta)$ is the Legendre function of second order, A_2 is the degree of alignment, defined later by Eq. (5), and W_L is the total intensity of each x-ray line and is proportional to the total L_3-hole production cross section and to the radiative transition probability.

Therefore, the intensity ratio $L\alpha/L_l$ is given by

$$\frac{L\alpha_{1,2}}{L_l}(\theta) = \frac{W_{L\alpha_1}(\theta)+W_{L\alpha_2}(\theta)}{W_{L_l}(\theta)} = \frac{\Gamma^{L\alpha_1}(1+\frac{1}{10}A_2P_2)+\Gamma^{L\alpha_2}(1-\frac{2}{5}A_2P_2)}{\Gamma^{L_l}(1+\frac{1}{2}A_2P_2)}, \qquad (2)$$

where $\Gamma^{L\alpha,l}$ are the radiative widths for transitions $L_{\alpha,l}$.

At $\theta = 90°$, where the measurement was carried out, this equation becomes

$$\frac{L\alpha_{1,2}}{L_l} = \frac{\Gamma^{L\alpha_1}+\Gamma^{L\alpha_2}}{\Gamma^{L_l}} \times\left[1+\left(1-\frac{5\Gamma^{L\alpha_1}}{4(\Gamma^{L\alpha_1}+\Gamma^{L\alpha_2})}\right)\tfrac{1}{5}A_2\right]/(1-\tfrac{1}{4}A_2). \qquad (3)$$

Assuming $\frac{1}{4}A_2 \ll 1$ and taking $\Gamma^{L\alpha_2}/\Gamma^{L\alpha_1} = 1/9$, which is obtained by using hydrogenlike wave functions for the $3d$ and $2p$ states,[18] the intensity ratio becomes

$$\frac{L\alpha_{1,2}}{L_l} \approx \frac{\Gamma^{L\alpha_1}+\Gamma^{L\alpha_2}}{\Gamma^{L_l}}(1+0.225A_2). \qquad (4)$$

Thus the ratio $L\alpha/L_l$ is a function of the degree of alignment A_2 as well as of the radiative transition probability. The quantity A_2, as a function of the L_3-hole production cross section $\sigma^h_{L_3}(m)$, is expressed by

$$A_2 = \frac{\sigma^h_{L_3}(m=\frac{3}{2})-\sigma^h_{L_3}(m=\frac{1}{2})}{\sigma^h_{L_3}(m=\frac{3}{2})+\sigma^h_{L_3}(m=\frac{1}{2})}, \qquad (5)$$

where m is the absolute value of the magnetic quantum number taking the incident direction as the z axis. Moreover, $\sigma^h_{L_3}(m)$ is related to the ionization cross section by

$$\sigma^i_{L_3}(m=\tfrac{3}{2}) = \sigma^i_{L_3}(m=\tfrac{3}{2}) + \tfrac{1}{2}(f_{13}+f_{12}\cdot f_{23})\sigma^i_{L_1} + \tfrac{1}{2}f_{23}\cdot\sigma^i_{L_2},$$
$$\sigma^i_{L_3}(m=\tfrac{1}{2}) = \sigma^i_{L_3}(m=\tfrac{1}{2}) + \tfrac{1}{2}(f_{13}+f_{14}\cdot f_{23})\sigma^i_{L_1} + \tfrac{1}{2}f_{23}\cdot\sigma^i_{L_2}. \qquad (6)$$

Here $\sigma^i_{L_3}(m)$ is the ionization cross section for the two L_3 electrons in each magnetic substate, $\sigma^i_{L_1}$ and $\sigma^i_{L_2}$ are total ionization cross sections for the L_1 and L_2 electrons, and the f's are Coster-Kronig transition probabilities.

From Eqs. (5) and (6) we obtain

$$A_2 = \frac{\sigma^i_{L_3}(m=\frac{3}{2})-\sigma^i_{L_3}(m=\frac{1}{2})}{(f_{13}+f_{12}\cdot f_{23})\sigma^i_{L_1}+f_{23}\cdot\sigma^i_{L_2}+\sigma^i_{L_3}}. \qquad (7)$$

The denominator of this equation can easily be obtained from the PWBA calculation of Choi *et al.*[19] using hydrogenlike wave functions.

The ionization cross section depending on m in the numerator has been calculated for electron impact by McFarlane,[13] and for heavy-charged particle impact it can be modified as

$$\sigma^i_{L_3}(m=\tfrac{3}{2}) = \sigma^i_{2p}(m=1),$$
$$\sigma^i_{L_3}(m=\tfrac{1}{2}) = \tfrac{1}{3}\sigma^i_{2p}(m=1)+\tfrac{2}{3}\sigma^i_{2p}(m=0). \qquad (8)$$

Here $\sigma^i_{2p}(m)$ is the ionization cross section without taking into account the spin of the electron and is calculated as[13]

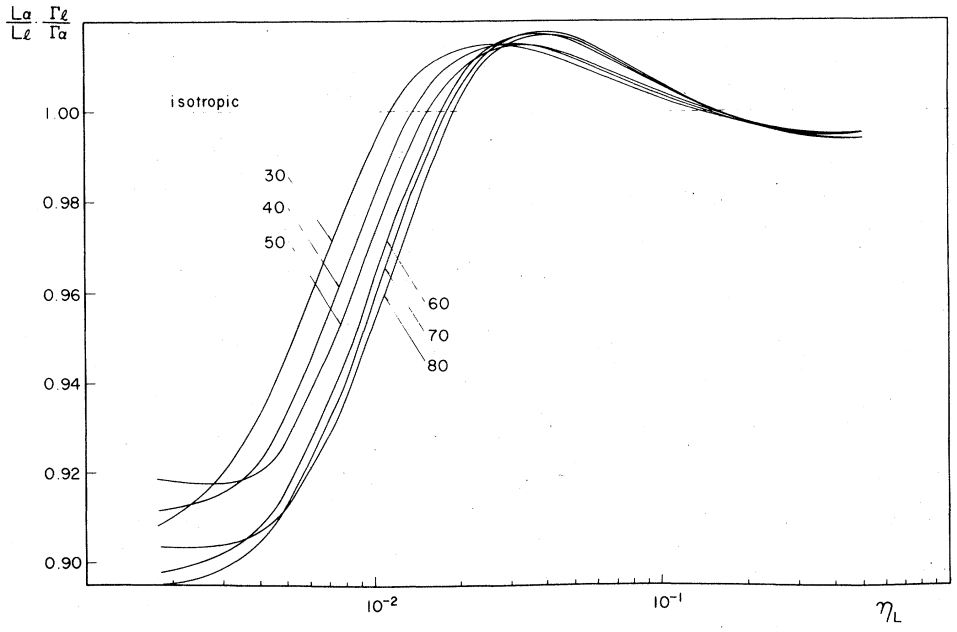

FIG. 4. Projectile-energy dependence of $L\alpha/L_l$ calculated from PWBA taking into account inner-shell alignment. The ordinate represents the value of ratio $L\alpha/L_l$ multiplied by the ratio of radiative transition probabilities $\Gamma_l/\Gamma\alpha$. The solid curves in the figure are labeled by the target atomic number.

$$\sigma_{2p}(m=0) = 8\pi Z_p^2 \frac{a_0^2}{Z_s^2}\left(\frac{e^2}{\hbar v}\right)^2 \int_{\theta/4}^{\infty} dW \int_{W^2/4\eta}^{\infty} \frac{dQ}{Q^2} \times[(1-\cos^2\lambda)F(\mu=1)+\cos^2\lambda\ F(\mu=0)],$$

$$\sigma_{2p}(m=1) = 8\pi Z_p^2 \frac{a_0^2}{Z_s^2}\left(\frac{e^2}{\hbar v}\right)^2 \int_{\theta/4}^{\infty} dW \int_{W^2/4\eta}^{\infty} \frac{dQ}{Q^2} \times\left[\frac{1+\cos^2\lambda}{2}F(\mu=1)+\frac{1-\cos^2\lambda}{2} \times F(\mu=0)\right], \quad (9)$$

where Z_p is the projectile atomic number, Z_s is the effective-target atomic number for the $2p$ subshell, a_0 is the Bohr radius, v is the projectile velocity, θ is the screening coefficient, W is the transfer energy in units of Z_s^2 Ry, Q is the square of the transfer momentum in units of $Z_s^2 a_0^{-2}$, μ is the magnetic quantum number taken with respect to the direction of the transfer momentum, and $\eta = (\hbar v/e^2)^2/Z_s^2$. Furthermore, λ is the angle between the incident beam and the transfer momentum and is given by

$$\cos^2\lambda = W^2/4Q\eta\,, \quad (10)$$

and $F(\mu=0)$ and $F(\mu=1)$ represent the ionization probability coefficients in the coordinate taking the direction of the transfer momentum as the z axis, and are calculated using the method of integral calculations involving confluent hypergeometric functions as[20]

$$F(\mu=0) = A(Q,k)\left[\frac{9}{4}Q^4 - \left(\frac{17}{12}+\frac{11}{3}k^2\right)Q^3 + \left(\frac{109}{480}+\frac{1}{12}k^2+\frac{7}{10}k^4\right)Q^2 + \left(\frac{17}{320}+\frac{111}{240}k^2+\frac{23}{20}k^4+\frac{3}{5}k^6\right)Q + \left(\frac{23}{30\times512}+\frac{19}{30\times32}k^2+\frac{3}{32}k^4+\frac{11}{60}k^6+\frac{7}{60}k^8\right)\right], \quad (11)$$

$$F(\mu=1) = \frac{1}{4}A(Q,k)(k^2+1)\left[\frac{4}{3}Q^3+\left(\frac{11}{15}-\frac{12}{5}k^2\right)Q^2+\left(\frac{7}{60}+\frac{2}{3}k^2+\frac{4}{5}k^4\right)Q+\frac{1}{15\times16}+\frac{1}{20}k^2+\frac{1}{5}k^4+\frac{4}{15}k^6\right],$$

where

$$A(Q,k) = 2^4 Q \exp\left[-\frac{2}{k}\tan^{-1}\left(\frac{k}{Q-k^2+\frac{1}{4}}\right)\right] \Big/ \left\{(1-e^{-2\pi/k})[(Q-k^2+\tfrac{1}{4})^2+k^2]^5\right\} \quad (12)$$

and k^2 is the kinetic energy of an ejected electron and is related to the transfer energy W by

$$W = k^2 + \tfrac{1}{4}\,. \quad (13)$$

Thus it is found that the ratio $L\alpha/L_l$ measured at $\theta = 90°$ depends on the projectile energy through A_2 in Eq. (3). The results of the present calculations by Eq. (9) for target atoms $Z = 30$–80 are

TABLE I. Results of PWBA calculations of the degree of alignment A_2 in units of 10^{-2} [Eq. (7)] and the normalized intensity ratio $R=(L\alpha/L_l)(\Gamma_l/\Gamma\alpha)$ at 90°. Z is the target-atomic number and $\eta=(\hbar v/e^2)^2/Z_s^2$.

	$Z=30$		$Z=40$		$Z=50$	
η	A_2	R	A_2	R	A_2	R
0.0018	−45.39	0.9081	−43.50	0.9116	−39.73	0.9185
0.0036	−35.14	0.9272	−39.16	0.9196	−39.78	0.9185
0.0050	−25.37	0.9462	−31.68	0.9338	−34.54	0.9284
0.0070	−13.87	0.9698	−20.86	0.9553	−25.13	0.9467
0.0100	−3.224	0.9928	−8.703	0.9808	−12.79	0.9721
0.0150	4.028	1.0092	1.425	1.0032	−0.9673	0.9978
0.0200	6.112	1.0140	5.120	1.0117	3.918	1.0087
0.0300	6.319	1.0145	6.531	1.015	6.332	1.0145
0.0400	5.451	1.0125	5.963	1.0136	6.070	1.0139
0.0500	4.513	1.0103	5.084	1.0116	5.292	1.0121
0.0600	3.677	1.0084	4.219	1.0096	4.461	1.0102
0.0800	2.316	1.0053	2.766	1.0063	3.002	1.0068
0.100	1.291	1.0029	1.644	1.0037	1.856	1.0042
0.150	−0.3618	0.9992	−0.1865	0.9996	−0.0345	0.999
0.200	−1.278	0.9971	−1.210	0.9973	−1.102	0.9975
0.300	−2.082	0.9953	−2.128	0.9952	−2.074	0.9954
0.400	−2.277	0.9949	−2.370	0.9947	−2.348	0.9947
0.500	−2.225	0.9950	−2.339	0.9948	−2.337	0.9948
	$Z=60$		$Z=70$		$Z=80$	
η	A_2	R	A_2	R	A_2	R
0.0018	−51.23	0.8977	−52.76	0.8949	−47.87	0.9036
0.0036	−46.90	0.9054	−48.67	0.9022	−47.05	0.9051
0.0050	−40.30	0.9175	−42.40	0.9136	−42.44	0.9135
0.0070	−30.26	0.9366	−32.70	0.9318	−34.18	0.9290
0.0100	−17.32	0.9626	−19.76	0.9575	−21.96	0.9531
0.0150	−3.659	0.9918	−53.38	0.9881	−7.095	0.9843
0.0200	2.978	1.0068	2.090	1.0047	0.9946	1.0022
0.0300	7.187	1.0165	7.157	1.0164	6.695	1.0154
0.0400	7.429	1.0171	7.686	1.0177	7.412	1.0170
0.050	6.693	1.0153	7.029	1.0161	6.832	1.0157
0.060	5.749	1.0131	6.090	1.0139	5.944	1.0136
0.080	3.968	1.0090	4.255	1.0097	4.185	1.0095
0.100	2.525	1.0057	2.750	1.0062	2.742	1.0062
0.150	1.291	1.0003	0.236	1.0005	0.3260	1.0007
0.200	−1.217	0.9973	−1.180	0.9973	−0.1044	0.9976
0.300	−2.438	0.9945	−2.473	0.9945	−2.310	0.9948
0.400	−2.790	0.9938	−2.855	0.9936	−2.698	0.9940
0.500	−2.792	0.9938	−2.869	0.9936	−2.727	0.9939

shown in Fig. 4, where the ordinate shows the ratio $L\alpha/L_l$ multiplied by the ratio of radiative transition probabilities $\Gamma_l/\Gamma\alpha$; the numerical results are shown in Table I.

IV. COMPARISON BETWEEN EXPERIMENTAL RESULTS AND PWBA CALCULATIONS

The results of the PWBA calculations as expressed by Eq. (3), using radiative transition probabilities given by Scofield and Coster-Kronig coefficients given by McGuire, are shown in Figs. 2 and 3 for Sm and Ho, respectively, where they are compared with the present experimental results. The values of Coster-Kronig coefficients for Sm were obtained from an interpolation of McGuire's calculations. As seen in these figures, the agreement between the experimental results and the theoretical calculation is excellent, especially in the low-energy region. It is also found that the ratio $L\alpha/L_l$ has about the same value for proton impact as for ^{3}He-ion impact at the same projectile velocity. This indicates that the binding-energy effect and the multiple ionization process play no significant role in this energy dependence. This is in agreement with a theoretical

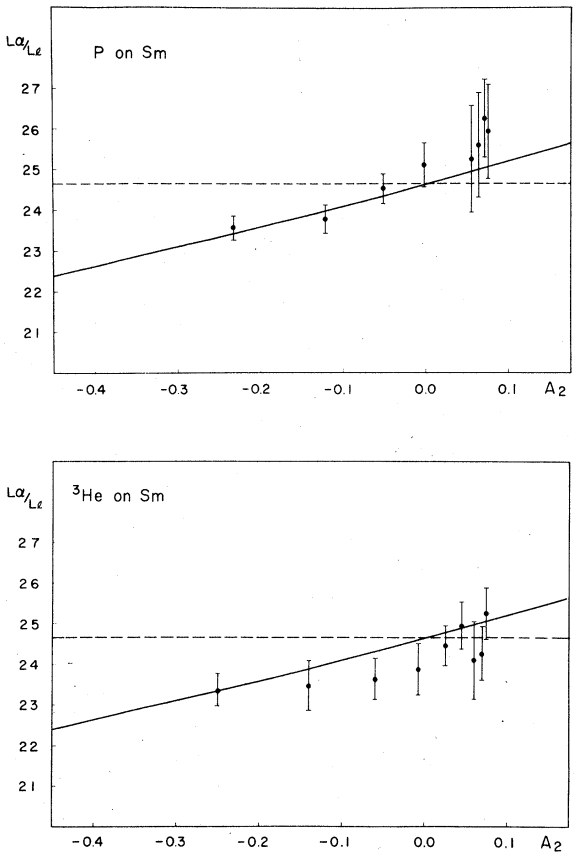

FIG. 5. Intensity ratio $L\alpha/L_l$ for proton and ^{3}He impacts on Sm as a function of A_2 [see Eq. (4)].

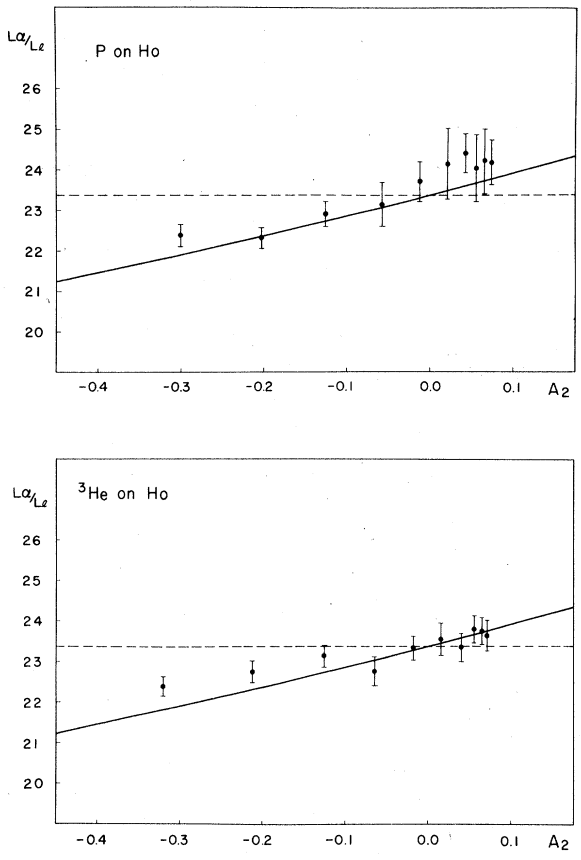

FIG. 6. Same as Fig. 5 except for Ho.

estimate using the method of Brandt and Lapicki[21] that indicates the difference between proton and ^{3}He-ion impact should be less than 1%. As shown by Eq. (4), the ratio $L\alpha/L_l$ is approximately expressed by a linear function of A_2, and this is supported by Figs. 5 and 6, where the ratio $L\alpha/L_l$ is plotted as a function of A_2.

In Figs. 7 and 8, experimental results on the $L\alpha/L_l$ ratio of Au (Ref. 10) and Pb (Ref. 7) bombarded by protons are compared with the present theoretical calculations. The agreement is quite satisfactory. The increase in the experimental values of the ratio in the lowest-energy region of Fig. 8 was not observed in the experiment of Chen *et al.*,[4] and might be due to reasons other than alignment. However, the experimental errors of the other results of Chen *et al.* are, in general, too large to compare with the present calculations.

V. DISCUSSION

As related in the preceding section, the projectile-energy dependence of the ratio $L\alpha/L_l$, observed experimentally, is well described by inner-shell alignment. The ionization process may theoretically be divided into contributions from close and distant collisions. In the low-energy region of $\eta < \frac{1}{4}\theta$, close collisions mainly contribute to the ionization, whereas in the region of $\eta > \frac{1}{4}\theta$ both close and distant collisions contribute nearly equally to the ionization cross section.

As seen from the incident direction of the projectile, the distribution of $2p$-state electrons having $m=0$ concentrates in the central region along the axis, while the electrons having $m=1$ are distributed in a ring of the radius of the electron orbital. On the other hand, the most probable impact parameter contributing to the ionization increases as the incident energy increases. In the low projectile-energy region, $2p$ electrons having $m=0$ are more likely to be ionized [namely, $\sigma_{2p}(m=1) < \sigma_{2p}(m=0)$], and therefore A_2 becomes negative. In the energy region of $\eta > \frac{1}{16}\theta^2$, electrons having $m=1$ are more likely to be ionized, and A_2 becomes positive. In addition, in the energy region of $\eta \approx \frac{1}{4}\theta$, the transfer momentum lies

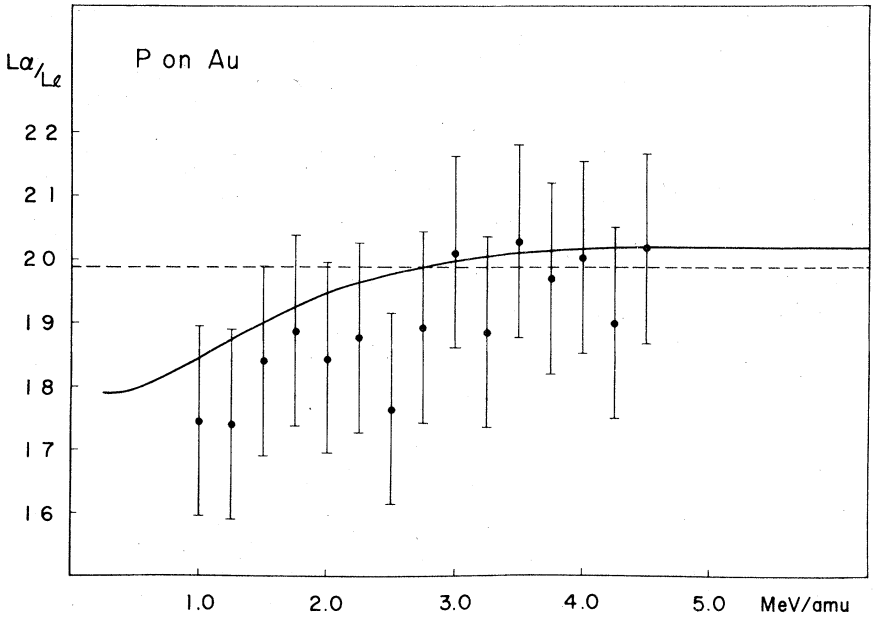

FIG. 7. Experimental results on $L\alpha/L_l$ (Ref. 10) for Au are compared with the present calculations shown by the solid line. Dashed line represents $\Gamma^{L\alpha}/\Gamma^{L_l}$ calculated by Scofield.

in the beam direction and the ionization of $m=0$ electrons, which oscillate along the beam axis, becomes effective and A_2 becomes negative. In the high-energy region, the transfer momentum becomes perpendicular to the beam direction and the ionization of $m=1$ electrons, which oscillate perpendicular to the axis, is expected to be effective and A_2 becomes positive.

In the present experiment little difference between the projectile-energy dependence of $L\alpha/L_l$ was found in proton and ^{3}He-ion impacts, over the energy range 0.75–3 MeV/amu. This fact might show that the ratio $L\alpha/L_l$ is not affected by such effects as Coulomb deflection, change of binding energy, and multiple ionization, all of which can introduce a projectile-energy dependence into the radiative transition probability, thereby giving rise to a difference between the energy dependence in proton and ^{3}He-ion impacts. According to the experimental results of Awaya *et al.*,[22]

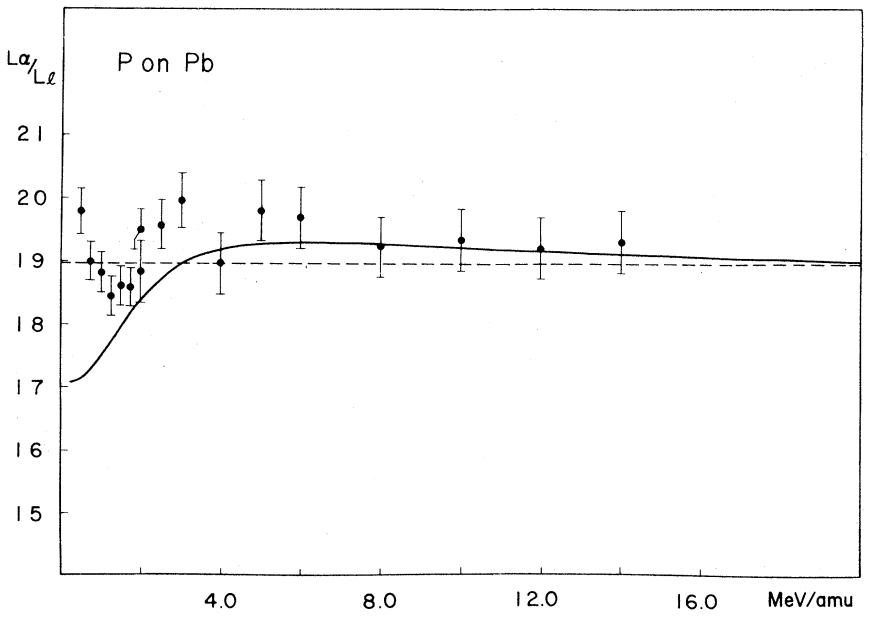

FIG. 8. Same as Fig. 7 except for Pb (Ref. 7).

where the ratios $L\alpha/L_l$ for Lu and Pb by α-particle impact were compard with those by nitrogen-ion impact, the contribution from the multiple ionization process is very small and can be neglected. However, in cases of very light atoms these effects might become important, as Rødbro *et al.*[16] have reported some differences between the values of A_2 obtained from measurements of Auger electrons emitted following Mg L_3-shell ionization by proton and ^{3}He-ion impacts.

VI. SUMMARY

The present experimental results on the $L\alpha/L_l$ ratio for Sm and Ho bombarded by protons and ^{3}He ions, together with the previous results for Au and Pb, were compared with PWBA calculations taking into account inner-shell alignment. Over the incident-energy range 0.5–5 MeV/amu it was found that the $L\alpha/L_l$ ratio does not depend on the projectile charge, and the projectile-energy dependence was explained in terms of the alignment of $2p_{3/2}$ vacancy states.

In order to obtain further and conclusive evidence for inner-shell alignment, precise measurements of the angular distribution of $L\alpha$ and L_l x rays are highly desirable.

ACKNOWLEDGMENT

The authors would like to express their sincere gratitude to M. Kato for his operation of the Van de Graaff generator throughout the experiment.

*Present address: The Institute of Physical and Chemical Research, Wako 351 Satima, Japan.

[1]D. A. Close, R. C. Bearse, J. J. Malanify, and C. J. Umbarger, Phys. Rev. A 8, 1873 (1973).
[2]F. Abrath and T. J. Gray, Phys. Rev. A 9, 682 (1974).
[3]R. Akselsson and T. B. Johansson, Z. Phys. 266, 245 (1974).
[4]J. R. Chen, J. D. Reber, D. J. Ellis, and T. E. Miller, Phys. Rev. A 13, 941 (1976).
[5]J. H. Scofield, Phys. Rev. 179, 9 (1969).
[6]J. H. Scofield, At. Data Nucl. Data Tables 14, 121 (1974).
[7]C. E. Busch, A. B. Baskin, P. H. Nettles, S. M. Shafroth, and A. W. Waltner, Phys. Rev. A 7, 1601 (1973).
[8]H. Tawara, K. Ishii, S. Morita, H. Kaji, C. N. Hsu, and T. Shiokawa, Phys. Rev. A 9, 1617 (1974).
[9]K. Ishii, S. Morita, H. Tawara, H. Kaji, and T. Shiokawa, Phys. Rev. A 10, 774 (1974).
[10]H. Tawara, K. Ishii, S. Morita, H. Kaji, and T. Shiokawa, Phys. Rev. A 11, 1560 (1975).
[11]W. Mehlhorn, Phys. Lett. 26A, 166 (1968).
[12]B. Cleff and W. Mehlhorn, J. Phys. B 7, 593 (1974).
[13]S. C. McFarlane, J. Phys. B 5 1906 (1972).
[14]E. G. Berezhko and N. M. Kabachnik, J. Phys. B 10, 2467 (1977).
[15]J. Hrdý, A. Henins, and J. A. Bearden, Phys. Rev. A 2, 1708 (1970).
[16]M. Rødbro, R. Dubois, and V. Schmidt (unpublished).
[17]E. G. Berezhko, N. M. Kabachnik, and V. V. Sizov, J. Phys. B 11, L421 (1978).
[18]H. A. Bethe and E. E. Salpeter, *Quantum Mechanics of One- and Two-Electron Atoms* (Plenum, New York, 1977), p. 273, Eq. (64.13).
[19]B. H. Choi, E. Merzbacher, and G. S. Khandelwal, At. Data 5, 291 (1973).
[20]L. D. Landau and E. M. Lifshitz, *Quantum Mechanics, Non-Relativistic Theory*, translated by J. B. Sykes and J. S. Bell (Pergamon, Oxford, 1965), p. 579.
[21]W. Brandt and G. Lapicki, Phys. Rev. A 10, 474 (1974).
[22]Y. Awaya, K. Izumo, T. Hamada, M. Okano, T. Takahashi, A. Hashizume, T. Tendow, and T. Kato, Phys. Rev. A 13, 992 (1976).